Available online at www.sciencedirect.com
ScienceDirect
Journal of Nuclear Materials 372 (2008) 171–176
journal of nuclear materials
www.elsevier.com/locate/jnucmat

Computer simulation of point defects in plutonium using MEAM potentials

L. Berlu [a], G. Jomard [b,*], G. Rosa [a], P. Faure [a]

[a] CEA Valduc, F-21120 Is Sur Tille, France
[b] CEA – Bruyères le Châtel, F-91680 Bruyères le Châtel, France

Received 17 May 2006; accepted 13 November 2006

Abstract

The zero-pressure formation energies of interstitials, vacancies and vacancies clusters have been calculated in face-centered-cubic plutonium using two versions of modified embedded atom potentials. Activation energies of interstitials and single vacancies have also been evaluated. Results for formation and migration energies are very sensitive to the analytical expression of the potential. Energy values are discussed in the context of plutonium self-irradiation simulations. Results give an explanation for defect microstructures composition and stability in thermalized displacements cascades.

1. Introduction

The radioactivity of plutonium is expressed essentially through α decay leading to the formation of uranium and helium nuclei. These particles carry a high energy and are responsible for collision sequences which create numerous point defects in the metal structure [1]. Such defects diffuse through the crystal, recombine with each other, eventually form clusters, and are responsible for modifications of macroscopic material properties. Experimental studies of the impact of self-irradiation on the long term evolution of Pu-based materials is limited by the radioactivity and toxicity of the samples. Consequently, computer simulations might be an alternative to experiments and notably help to determine specific properties of defect populations and their evolution with time [2]. To understand self-irradiation effects in plutonium alloys, we have developed a multi-scale modelling program which consists of a sequence of computer simulation methods ranging from first-principles and classical molecular dynamics (MD) to methods such as mesoscopic Monte Carlo (MMC) and rate equations (RE). The basic idea of this project is that input data of a specific scale code are obtained from the previous ones. The α decay of plutonium is simulated by MD through displacements cascades. For example, the configurations of the created defects are then used as input data for simulations at the mesoscopic scale (i.e. MMC and RE) to describe longer time scale evolution. However, the number and spatial repartition of point defects are not enough to run mesoscopic methods, which require also intrinsic defects properties such as formation and migration energies. Such calculations are usually performed by ab initio or MD simulations. However, even the best density functional theory methods have problems accurately describing the δ phase of Pu and are very computational time consuming [3]. So in this work, we have tried to explore defects properties in δ-Pu using the well-established MEAM many-body potential of Baskes. In the present paper, zero-pressure formation energies of interstitials, vacancies, di-vacancies and tri-vacancies; and migration energies of interstitials and vacancies are presented.

2. MEAM potential functions and definitions

Since pair-wise potentials have shown their inefficiency to describe metal structures, many-body potentials have

* Corresponding author.
E-mail address: gerald.jomard@cea.fr (G. Jomard).

0022-3115/$ - see front matter © 2007 Elsevier B.V. All rights reserved.
doi:10.1016/j.jnucmat.2006.11.016

been developed. In a previous work, an EAM interatomic potential was used to simulate MD displacement cascades in FCC δ phase of plutonium [4]. However, it is well known that the EAM formalism is not able to reproduce the complex behaviour of plutonium. For example, EAM formalism imposing $C_{12} \geqslant C_{44}$ fails to predict the negative Cauchy pressure $\frac{1}{2}(C_{12} - C_{44})$ of Pu [5]. This highlights the necessity to use a potential more representative of atomic interactions. In that way, Baskes et al. modified the Embedded Atom Method in order to extend its application to materials exhibiting a strong directional bonding [6–8]. Then for the calculations presented here, we used the MEAM potential developed for plutonium by Baskes [9–11]. In Table 1 we present the predicted elastic constants by both the EAM potential of Pochet and by the MEAM one of Baskes [4,9]. One can clearly notice that the EAM potential predicts a wrong slightly positive Cauchy pressure. The basic idea of MEAM is to introduce an angular dependency in the formulation of the background electron density which is purely spherical in EAM. This density is a combination of partial electron densities (noted $\rho^{(l)}$) that contain this dependency. The way of combining these $\rho^{(l)}$ is not unique and several expressions have been proposed [12]. Among them, the following form that can be widely used without numerical errors is considered in the present work:

$$\bar{\rho} = \rho^{(0)} G(\Gamma), \tag{1}$$

where $G(\Gamma) = \frac{2}{1+\exp -\Gamma}$ with Γ the combination of angular electronic densities given by

$$\Gamma = \sum_{l=1}^{3} t^{(l)} (\rho^{(l)}/\rho^{(0)})^2, \tag{2}$$

where $\rho^{(l)}$ are the partial electronic densities and $t^{(l)}$ their weights in the total density. We must point out that even if we have used the set of parameters fitted by Baskes, our formulation differs from the original one because for plutonium, Baskes has used the $G(\Gamma) = \sqrt{(1+\Gamma)}$ expression. But the later has shown in a complete study on Ni that the form of $G(\Gamma)$ does not strongly affect defect properties [12]. Moreover, as shown in previous works, the choice made for $G(\Gamma)$ does not perturb the ability of the potential to reproduce elastic constants of plutonium [11,13].

Table 1
Calculated structural and elastic properties of δ-Pu with the EAM potential of Pochet and the MEAM one of Baskes

Properties	MEAM Baskes	EAM Pochet	Experimental
V_{eq} (Å^3)	25.1	25	24.9
B_0 (GPa)	29.3	30	29.9
C_{11} (GPa)	35.8	40.2	36.3
C_{12} (GPa)	25.8	24.8	26.4
C_{44} (GPa)	36.5	24.7	33.6
P_{Cauchy} (GPa)	−5.3	0.05	−3.6

For comparison, the corresponding experimental data from Ref. [19] are also tabulated.

For determining the formation energy of an n defect(s) configuration from a reference structure, we used the following usual definition:

$$E_f^{(n)} = E_{def}^{(n)} - \frac{N \pm n}{N} E_{ref}, \tag{3}$$

where $E_{def}^{(n)}$ is the n defect(s) configuration energy per atom, E_{ref} is the reference state energy per atom, N is the number of atoms in the reference state, n is the number of defects (+ sign is for interstitial defects and − for vacancies).

3. Method

To calculate the energetic properties of point defects we used the so-called supercell method. Special care has been taken in the case of interstitials defects that are highly mobile. Then at first, an atom was inserted near the center of the crystal in the required configuration. The initial temperature was set to 0 K, atomic motion came from excess of potential energy due to defects. The energy minimization was performed with the Beeler's algorithm in which velocity of atoms leaving a minimum is cancelled. The MD simulation was performed with a time step of 1 fs. To constrain interstitials to stay in the configuration of interest, the dynamics was stopped with a period of 400 steps, the barycenter of interstitials was replaced in its initial position and dumbells were aligned in the desired orientation. These operations were iterated until the energy changed by less than 1×10^{-6} eV. The entire supercell undergoes volume relaxation to produce the final zero-pressure configuration. These two stages were iterated until a stable minimum is obtained. Using this approach, the excess of force due to interstitials is relaxed over the crystal.

The same procedure has been applied for the calculation of vacancies formation energies. In this case the desired number of atoms was removed to construct the n vacancies defect.

Formation and migration energies of defects are obtained with accuracy better than 10 meV. Defects configurations studied in this paper are shown in Fig. 1. One can see that we have studied mono-, di- and tri-vacancies as well as various dumbells and single interstitials atoms (SIA).

In order to check the convergence of the point defects formation energies with respect to the size of the supercell, we have performed calculations with cells of 256, 2048 and 4000 atoms, respectively. The results of this procedure are summarized in Tables 2–5. We can notice that energetics of vacancy-type defects are already converged for a supercell containing 256 atoms. The situation is a little bit different in the case of mono- and di-interstitials which is not surprising since atomic relaxations are more important than for vacancies. One has to consider cells containing as much as 2048 atoms in order to achieve a convergence of about 0.01 eV on the formation energies. In the following we will thus refer to the results obtained for the 2048 atoms cells.

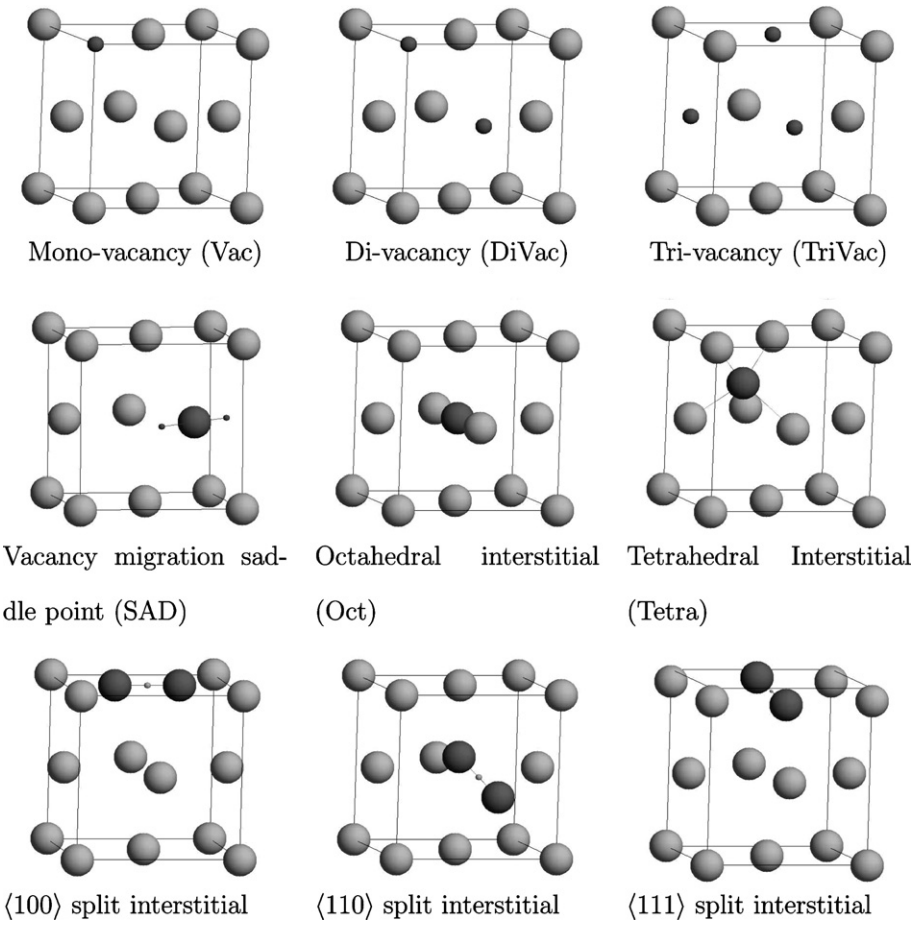

Fig. 1. Configurations of interstitials and vacancies structures. Abbreviations used in the following are indicated in brackets. Lightgrey spheres are FCC positions, Grey are interstitials atoms and small are vacant FCC sites.

Table 2
Interstitials formation energies

Configuration	⟨100⟩	⟨110⟩	⟨111⟩	Octahedral	Tetrahedral
E_f (eV) 256 atoms	0.56	1.66	1.29	0.82	3.40
E_f (eV) 2048 atoms	0.49	1.43	1.16	0.78	3.30
E_f (eV) 4000 atoms	0.49	1.44	1.17	0.79	3.30

Table 3
Vacancies configurations formation and cohesion[a] energies

Configuration	MonoVac	DiVac	TriVac	SAD
E_f (eV) 256 atoms	0.45	0.97	1.45	1.18
E_f (eV) 2048 atoms	0.45	0.96	1.45	1.19
E_f (eV) 4000 atoms	0.44	0.96	1.44	1.20
E_c (eV) 256 atoms	–	0.07	0.10	–
E_c (eV) 2048 atoms	–	0.06	0.10	–
E_c (eV) 4000 atoms	–	0.06	0.12	–

[a] The cohesion energy of an n defects cluster is defined as the difference of cluster formation energy minus n times the self-defect ones: $E_c^{(n)} = E_f^{(n)} - n \times E_f^{(1)}$.

Table 4
Interstitials formation energies calculated within the MEAM* potential

Configuration	⟨100⟩	⟨110⟩	⟨111⟩	Octahedral	Tetrahedral
E_f (eV) 256 atoms	1.71	2.36	2.59	1.84	3.76
E_f (eV) 2048 atoms	1.66	2.19	2.48	1.82	3.66
E_f (eV) 4000 atoms	1.66	2.19	2.47	1.82	3.66

Table 5
Vacancies configurations formation and cohesion energies calculated within the MEAM* potential

Configuration	MonoVac	DiVac	TriVac	SAD
E_f (eV) 256 atoms	0.53	1.10	1.61	1.47
E_f (eV) 2048 atoms	0.53	1.10	1.61	1.47
E_f (eV) 4000 atoms	0.53	1.10	1.61	1.47
E_c (eV) 256 atoms	–	0.04	0.02	–
E_c (eV) 2048 atoms	–	0.04	0.02	–
E_c (eV) 4000 atoms	–	0.04	0.02	–

The interstitials migration energy has been evaluated by performing MD calculations with a simulation cell containing one interstitial and with temperature ranging from 300 K to 800 K. The mean square displacement was plotted versus time and migration energy computed from Einstein and Arrhenius equations:

$$D(T) = \lim_{t\to\infty} \frac{\langle r^2\rangle_T}{6t}, \quad (4)$$

$$D(T) = D_0 \exp(-E_m/kT), \quad (5)$$

where T is the temperature, k is the Boltzmann constant, $\langle r^2\rangle_T$ is the mean square displacement at temperature T, t is the time of the MD, D_0 is the diffusivity constant and E_m is the migration energy.

Since vacancies migration rate is very small, the method used for interstitial migration energy would require MD lasting for microseconds. Such a simulation, even with a small number of atoms, would need considerable computational effort. Thus, vacancy migration energy has been evaluated from the difference of mono-vacancy formation energy and the minimization of the saddle point energy. Here, the saddle point was assumed to be an atom placed at the middle of two vacant first neighbours FCC sites (see SAD in Fig. 1), and the structure was relaxed as for interstitial. The activation energy was then obtained by

$$E_m^{Vac} = E_f^{SAD} - E_f^{Vac}, \quad (6)$$

where E_f^{SAD} is the saddle point energy and E_f^{Vac} the formation energy of a mono-vacancy.

4. Results

The interstitial formation energies are summarized in Table 2. The ⟨100⟩ dumbell was found to be the most stable configuration followed by the octahedral SIA. Other configurations are found to be largely less stable.

Fig. 2 shows a plot of the mean square displacement, $\langle r^2\rangle_T$, versus time and temperature. From the slope of linear interpolations of $\langle r^2\rangle_T \equiv f(t)$ for each temperature, and through Eqs. (4) and (5), the Fig. 3 was obtained and interstitial migration energy was found to be 0.079 eV.

The results obtained for vacancies configurations are reported in Table 3. The cohesion energy for di-vacancies and tri-vacancies was found to be positive. This means that, in this model, di-vacancies and tri-vacancies are less stable than isolated vacancies. From the saddle point and the mono-vacancy formation energies, using (6), vacancy migration energy was found to be 0.80 eV.

To understand the influence of interatomic potential on defects stability and radiation damage simulation results, the same calculations were performed with the so-called MEAM* potential corresponding to the MEAM potential with a sort of localization of the 5f electrons [14]. Indeed, the MEAM* potential is obtained by cancelling the coefficient $t^{(3)}$ in the combination of angular electronic densities $\Gamma = \sum_{l=1}^{3} t^{(l)}(\rho^{(l)}/\rho^{(0)})^2$. That corresponds to remove a sensitivity to inversion symmetry in the crystal structure which stabilizes the δ phase of Pu [11,15]. Consequently, the formation and migration energies of point defects increases (Tables 4 and 5).

5. Discussion

The migration energy calculated for interstitial is in good agreement with those of the literature. In [11] Valone et al. found 0.056 eV by MD calculations in pure Pu, and in [16,17] Fluss et al. estimated a value of about 0.1 eV from isochronal annealing experiments and kinetic Monte Carlo simulations in PuGa alloys. Note here that the MEAM parameters in [9,10] are relative to Ga-stabilized δ plutonium, so it is not surprising that results compare well with PuGa alloys defect properties. In displacement cascades

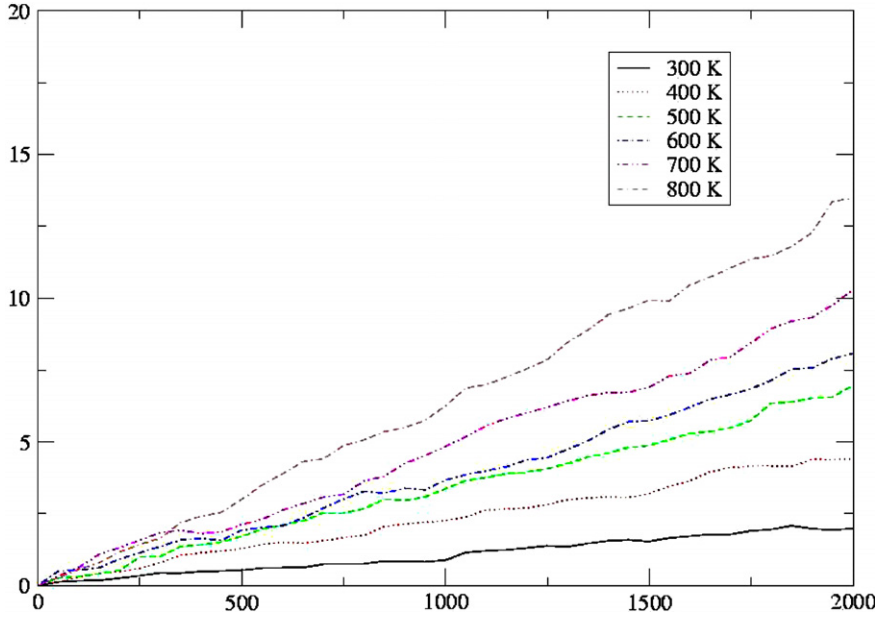

Fig. 2. Mean square displacement (Å^2) as a function of time (ps) and temperature (K).

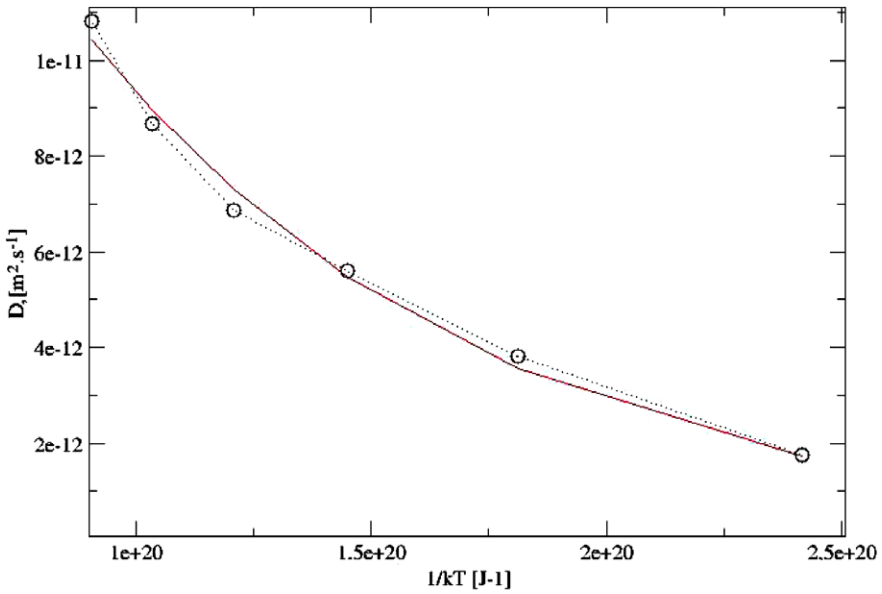

Fig. 3. Diffusion constant, D, (m^2s^{-1}) versus $1/kT$ (J^{-1}) form the measurement of the root mean square in simulation and Eqs. (4) and (5). Black open circle are points from simulation and solid line is the fit of simulation results with Eq. (5).

simulations, the predominant configuration of interstitial is the ⟨1 0 0⟩ split form in agreement with formation energies calculations [11,13,18].

For the calculation of vacancy migration energy, the jump path was assumed to be along ⟨1 0 0⟩ direction and no multi-jump, in concerted motion as observed by Uberuaga et al. in parallel replica simulations, has been considered [15]. Under these assumptions, the vacancy migration energy can be derived simply as the difference between formation energies of the saddle point and of the mono-vacancy. This very simple approach gives a value of 0.80 eV which is in good agreement with the single hop of Uberuaga et al. [15], but cannot be used to find the most frequent pathway. Furthermore, our result is in the range of values (0.7 ± 0.1) eV reported by Fluss and co-workers [16,17]. The sum of the formation and migration mono-vacancy energies is 1.25 eV. This is very close to results from [11,17] and references therein. Vacancy formation energies range from 0.45 to 1.45 eV for the mono-vacancy, di-vacancy and tri-vacancy. These values imply that small vacancy clusters are not stable in the model. This result is consistent with the microstructure of defects obtained by displacements cascades simulations in plutonium [13]. However, the positive cohesive energy of di-vacancies is not in agreement with density functional calculations by Robert et al. [3]. First-principles results could then be used to develop more realistic interatomic potentials for plutonium as suggested by Robert.

The calculations performed in MEAM* show that vacancy clusters are as stable as isolated vacancies. The SAD energy is found to be 1.47 eV giving 0.94 eV for the vacancy migration energy. Interstitials formation energies increased by ~1.0 eV. These point defects energies prove that 5f electrons have an important effect on the potential surface energy. As described by Valone et al. [11], the MEAM potential is a multi-phase potential with numerous local minima surrounding FCC positions. These minima correspond, amongst other configurations, to the monoclinic α phase of plutonium. Displaced atoms can be captured in these minima. Thus, the ability of atoms to move is reduced with MEAM potential. Interstitial point defects are stabilized and their annealing with neighbouring vacancies is prevented. In MEAM* things look different: 5f electrons contribution is removed, monoclinic minima are smoothed and interstitial positions destabilized. The consequence would be a more usual FCC behaviour of displacements cascade defects microstructures which is in agreement with recent results obtained by Kubota et al. comparing displacements cascades simulation within MEAM and MEAM* [14].

6. Conclusion

In this paper, formation and migration energies of point defects have been computed in δ plutonium using MEAM potentials. Results are in good agreement both with experimental and computational values already published. Comparisons with first-principles calculations show that MEAM potential should be improved to describe more realistic interactions.

The point defects energies are discussed in terms of radiation damage stability. The 5f electrons contribution to the density in the potential is shown to lead to a stabilization of point defects positions. This behaviour is attributed to a consequence of the presence of many local minima in the surrounding of FCC positions within the MEAM used potential.

References

[1] W.G. Wolfer, Los Alamos Sci. 26 (2000) 275.
[2] N. Baclet, P. Faure, G. Rosa, B. Ravat, L. Jolly, B. Oudot, L. Berlu, V. Klosek, J.L. Flament, G. Jomard, in: R. Avares, N.D. Brian, I. May (Eds.), Recent Advances in Actinides Science, Royal Society of Chemistry, 2006.
[3] G. Robert, A. Pasturel, B. Siberchicot, Europhys. Lett. 71 (2005) 41.
[4] P. Pochet, Nucl. Instrum. and Meth. B 202 (2003) 82.
[5] M.S. Daw, M.I. Baskes, Phys. Rev. B 29 (1984) 6443.
[6] M. Baskes, Phys. Rev. Lett. 59 (1987) 2666.
[7] M. Baskes, J. Nelson, A. Wright, Phys. Rev. B 40 (1989) 6085.
[8] M. Baskes, Phys. Rev. B 46 (1992) 2727.
[9] M.I. Baskes, Phys. Rev. B 62 (2000) 15532.
[10] M.I. Baskes, K. Muralidharan, M. Stan, S.M. Valone, F.J. Cherne, JOM (September) (2003) 41.
[11] S.M. Valone, M.I. Baskes, M. Stam, T.E. Mitchell, A.C. Lawson, K.E. Sickafus, J. Nucl. Mater. 324 (2004) 41.
[12] M.I. Baskes, Mater. Chem. Phys. 50 (1997) 152.
[13] L. Berlu, G. Rosa, P. Faure, N. Baclet, G. Jomard, in: J. Sarrao, A. Schwartz, M. Antonio, P. Burns, R. Haire, H. Nische (Eds.), Basis Science, Application and Technology, Mater. Res. Symp. Proc., vol. 893, PA, Warrendale, 2005.
[14] A. Kubota, W.G. Wolfer, M.J. Caturla, in: 35ième journée des actinides, Vienna, Austria, 2005.
[15] B.P. Uberuaga, S.M. Valone, S.M.Valone, M.I. Baskes, A.F. Voter, in: Plutonium Futures, 2003, p. 213.
[16] B.D. Wirth, A.J. Schwartz, M.J. Fluss, M.J. Caturla, M.A. Wall, W.G. Wolfer, MRS Bull. 26 (2001) 679.
[17] M.J. Fluss, B.D. Wirth, M. Wall, T.E. Felter, M.J. Caturla, A. Kubota, T.D. de la Rubia, J. Alloys Compd. 368 (2004) 62.
[18] G. Jomard, P.M. Anglade, in: Proceedings of the Third International Conference on Computational Modelling and Simulation of Materials, Acireale, Sicily, Italy, 2004.
[19] O. WickPlutonium Handbook: A Guide to the Technology, vols. I and II, The American Nuclear Society, La Grange park, IL, 1980.